Journal of Pharmacokinetics and Biopharmaceutics, Vol. 24, No. 6, 1996

Use of Parallel Erlang Density Functions to Analyze First-Pass Pulmonary Uptake of Multiple Indicators in Dogs[1]

T. C. Krejcie,[2,4] J. A. Jacquez,[3] M. J. Avram,[2] C. U. Niemann,[2] C. A. Shanks,[2] and T. K. Henthorn[2]

Received October 24, 1995—Final January 8, 1997

The gamma and Erlang density functions describe a large class of lagged, right-skewed distributions. The Erlang distribution has been shown to be the analytic solution for a chain of compartments with identical rate constants. This relationship makes it useful for the analysis of first-pass pulmonary drug uptake data following intravenous bolus administration and the incorporation of this analysis into an overall systemic drug disposition model. However, others have shown that one Erlang density function characterizes the residence time distribution of solutes in single tissues with significant systematic error. We propose a model of two Erlang density functions in parallel that does characterize well the arterial appearance of indocyanine green, antipyrine, and alfentanil administered simultaneously by right atrial bolus injection. We derive the equations that permit calculation of the higher order moments of a system consisting of two parallel Erlang density functions and use the results of these calculations from the data for all three indicators to estimate pulmonary capillary blood volume and mean transit time in the dog.

KEY WORDS: indocyanine green; antipyrine; alfentanil; tissue distribution; physiologic models; dogs; pulmonary uptake; pulmonary capillary blood volume; pulmonary capillary transit time.

INTRODUCTION

The drug concentration vs. time profile of the initial arterial appearance, after rapid intravenous (bolus) administration, of drugs that interact strongly with pulmonary tissue (e.g., basic amines) is significantly different

[1]Supported in part by the National Institute of General Medical Sciences, RO1-GM-43776, RO1-GM-47502, and PO1-GM-47819.
[2]Department of Anesthesiology, Northwestern University Medical School, CH-W139, 303 E. Chicago Avenue, Chicago, Illinois 60611-3008.
[3]Department of Physiology, University of Michigan, 7808 Medical Sciences II, Ann Arbor, Michigan 48109-0622.
[4]To whom correspondence should be addressed.

0090-466X/96/1200-0569$09.50/0

from that of drugs which have no such strong interaction (1,2). Quantitation of this tissue-drug interaction requires a multiple indicator dilution technique to account for the kinetic events representing intravascular and tissue water effects (3).

A multiple indicator dilution technique using albumin, diazepam, and alfentanil as markers has been used by Audi *et al.* to estimate pulmonary capillary kinetics in isolated perfused dog and rabbit lungs (4,5). The technique of Audi *et al.* utilizes the higher order moments of the transit time density function to describe the indicator outflow concentrations from pulmonary tissue.

The synthetic opioid alfentanil is a basic amine with the most rapid onset of effect of any of the opioid drugs, hence variability in its pulmonary disposition may contribute to interindividual differences in drug response. We report the results of a study of the pulmonary uptake of alfentanil conducted in the intact dog using a multiple indicator dilution technique in which indocyanine green (ICG) and antipyrine are used to account for the kinetic events representing intravascular and tissue water effects, respectively. We propose a model in which the arterial appearance history of each of the multiple indicators is characterized by two parallel gamma distributions, with different transit parameters, that improves upon the basic (single) gamma distribution model and upon the single pathway central (pulmonary) circulation we have used previously (6,7).

The gamma pulmonary disposition model used in the present study is equivalent to the sum of two parallel Erlang frequency distributions in which the n parameters of the gamma distributions are rounded to the nearest integer value. We will show how this relationship can be exploited for the construction of compartmental models of *in vivo* drug distribution that include precise characterization of pulmonary drug uptake and nearly continuous arterial drug concentration sampling. In addition, the variables from either the gamma or Erlang distributions can be used to calculate directly the higher order moments. We used the higher order moments describing our data to estimate pulmonary capillary kinetics in order to assess the ability of this proposed methodology to deal with the potentially confounding influence of recirculation on pulmonary kinetics derived *in vivo*.

METHODS

Following Institutional Animal Care and Use Committee approval, we studied four conditioned, heart worm-free male mongrel dogs that were one to three years old and weighed 22 to 30 kg. Anesthesia was induced with methohexital (15 mg/kg) administered through an 18 g Teflon® catheter in a foreleg vein. After the trachea was intubated with a 9 mm tracheal tube,

controlled, positive-pressure ventilation was instituted and maintained throughout the experiment with an inspired mixture of 2% halothane in oxygen. A 16 g, 2 in Teflon® catheter was placed percutaneously in a femoral artery and a 7 Fr flow-directed pulmonary arterial catheter (Baxter-Edwards 93A-140-7F, with a proximal port at 20 cm) was positioned through an 8 Fr introducer that was placed percutaneously in the right external jugular vein.

At the onset of the study (time $t = -0.05$ min), ICG (5 mg in 1 ml of diluent), antipyrine (25 mg in one ml), and alfentanil (1 mg in 2 ml) (Janssen Pharmaceutica, New Jersey), were placed in a leading length of tubing and injected within one second through the proximal pulmonary artery catheter port and flushed in with 10 ml of 0.9% saline solution. Three milliliter arterial blood samples were collected every 0.05 min for the first minute and every 0.1 min for the next minute using a computer-controlled roller pump (Masterflex, Cole-Parmer, Chicago, Illinois) with polyvinyl tubing having a total deadspace volume of 3 ml (in order to both minimize total collection system volume and to match the volume collected for each sample), running at 1 ml/sec for the first minute and 0.5 ml/sec for the next minute, and a chromatography fraction collector (Model 203, Gilson, Middleton, Wisconsin). This collection system was actuated just prior to the injection time ($t = -0.05$ min) and blood withdrawn before time $t = 0$ was discarded in order to correct the discrepancy created by the catheter transit delay. Huang *et al.* (8) have indicated that laminar flow within such catheter systems may affect results only when the system's flow to volume ratio is much smaller than ours. Tests performed in our laboratory on our system confirms these observations and that deviation from true plug-flow is trivial. Subsequent arterial blood samples were drawn manually at 0.5 min intervals to 4 min. Dogs were euthanatized by intravenous injection of saturated KCl solution while anesthetized at the conclusion of the study.

Hematocrits were determined on blood obtained before and at one and two minutes after drug injection. Plasma drug concentrations were converted to blood concentrations to facilitate the estimation of the contributions of blood flow and transcapillary diffusion to intercompartmental clearance and to allow estimation of intravascular volumes.

Plasma ICG concentrations of all samples were measured on the day of the study by HPLC (9). This method has been modified in our laboratory by the use of two detector/integrator pairs in series, one monitoring absorbance of desmethyldiazepam (the internal standard) at 254 nm and one monitoring absorbance of ICG at 786 nm (6). This produces a linear ICG measurement range of 0.2 μg/ml to 20.00 μg/ml with coefficients of variation of 5% or less. Plasma ICG concentrations were converted to blood concentrations by multiplying plasma ICG concentrations by one minus the hematocrit, as ICG does not partition into erythrocytes.

Plasma antipyrine concentrations of all samples were measured in duplicate using an HPLC technique similar to our barbiturate assay (7,10). Plasma samples were extracted in duplicate with solid phase extraction columns using 4-aminoantipyrine as the internal standard. Samples were eluted isocratically from a Radial-Pak C18 cartridge (Waters Associates, Milford, Massachusetts) and absorbance monitored at 254 nm. The antipyrine method is linear from 0.10 μg/ml to 10.00 μg/ml, with coefficients of variation of 5% or less.

Plasma alfentanil concentrations were measured using an adaptation of the GC-NPD technique of Björkman and Stanski (11). Plasma samples were extracted in duplicate with solid phase extraction columns using fentanyl as the internal standard. The assay has sensitivity over a linear range of 50 ng/ml to 5000 ng/ml, with coefficients of variation of 7% or less throughout the range.

Data Analysis

In general, models that describe drug concentration histories measured at an organ outflow, following impulse inflow administration, must be unimodal, asymmetric and right-skewed. Compartmental flow models are in this class and give, among others, the Erlang density function. Figure 1a shows the form of a tanks-in-series or linear chain of n identical compartments with exiting rate constant k. The solution for a linear chain obtained by successive integration for the rate of exit from compartment n is given by:

$$f(t)=\frac{k^n \cdot t^{n-1}}{(n-1)!} \cdot e^{-kt} \tag{1}$$

where

$$\int_0^\infty f(t)\,dt=1 \tag{2}$$

This is an Erlang density function which is a special case of the gamma distribution function:

$$f(t)=\frac{k^n \cdot t^{n-1}}{\Gamma(n)} \cdot e^{-kt} \tag{3}$$

with n restricted to integer values. These functions describe a drug or indicator concentration history $C(t)$:

$$C(t)=A \cdot f(t) \tag{4}$$

where A is the area under the plasma or blood drug concentration vs. time relationship (AUC or zeroeth moment). Higher order moments describe the

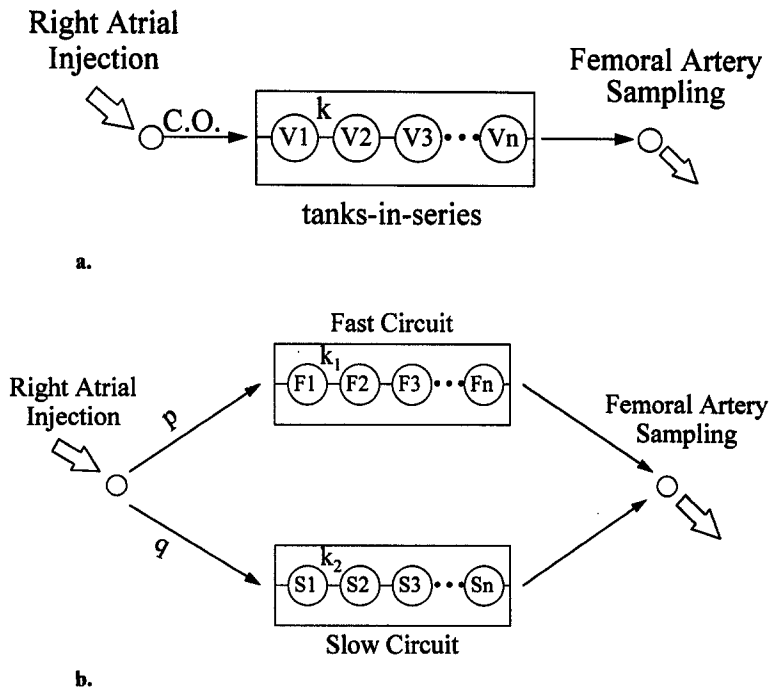

Fig. 1. (a) Schematic of a flow-through system modeled as a linear chain (or tanks-in-series) in which compartments (V1) are linked in series by transfer rate constants (k) of identical value are interposed between the sites of administration and sampling. (b) Schematic of a flow-through system modeled as a pair of linear chains or (tanks-in-series) interposed between the sites of administration and sampling. Flow is divided between pathways p and q (shown as transfer constants of unequal size connoting differential apportionment of flow) each having a distinct number of compartments ($F1$, $S1$) and linked in series by transfer rate constants (k_1, k_2) that are unique to each pathway but identical within it.

characteristics of the concentration vs. time profile. The first moment estimates the mean transit time (mtt), the second central moment estimates the variance (σ^2), and the third central moment estimates the skewness (δ). Using the Erlang (gamma) function, which describes right-skewed, lagged distributions (e.g., single-pass drug concentration history), the higher order moments are easily calculated (using n and k from Eqs. (1) or (3)) as follows:

$$mtt = \frac{n}{k} \tag{5}$$

$$\sigma^2 = \frac{n}{k^2} \tag{6}$$

$$\delta = \frac{2 \cdot n}{k^3} \tag{7}$$

Cardiac output (*C.O.*, which is the flow through the central or pulmonary circulation) is estimated from the ICG (dye) dilution curve (12):

$$C.O. = \frac{\text{Dose}}{\text{AUC}} \tag{8}$$

The apparent distribution volume (Vd) between the right atrial injection site and the arterial sampling site can be estimated from:

$$Vd = mtt \cdot C.O. \tag{9}$$

For ICG, this Vd is an estimate of the central or thoracic plasma volume, which is also an estimate of central blood volume when it is divided by (1-Hct). For drugs or indicators that readily leave the intravascular space to partition into tissues, the difference between the intravascular volume (i.e., the Vd for ICG) and the Vd for the drug or indicator that distributes to tissue provides an estimate of the apparent pulmonary tissue volume.

Audi *et al.* have described a method of estimating pulmonary capillary blood volume using a multiple indicator dilution technique in which one indicator is an intravascular reference marker (e.g., ICG) and at least two other indicators which variably distribute to pulmonary tissue in a flow-limited manner (4,5). They reasoned that the different extravascular kinetics of these markers arise solely during their pulmonary capillary sojourns. In the present study, the two flow-limited markers used were antipyrine and alfentanil. Antipyrine has long been used as a flow-limited tissue distribution marker that provides an estimate of tissue water space, including that of the lung (13,14). Our previous work and that of others indicate that the tissue distribution of alfentanil is also largely flow limited (15,16).

From the respective outflow indicator concentration histories, the *mtt*, σ^2, and δ are estimated. The extravascular mtt_e, σ_e^2, and δ_e of the flow-limited markers (antipyrine and alfentanil) are derived by subtracting from the respective values for the drugs those values for the intravascular indicator (ICG) (4,5):

$$mtt_e = mtt_{drug} - mtt_{ICG} \tag{10}$$

$$\sigma_e^2 = \sigma_{drug}^2 - \sigma_{ICG}^2 \tag{11}$$

$$\delta_e = \delta_{drug} - \delta_{ICG} \tag{12}$$

Such extravascular kinetics of two or more markers can be used to solve, by an iterative, nonlinear, least squares estimation technique, the following equations (4):

$$\sigma_{ei}^2 = \left[\left(1 + \frac{mtt_{ei}}{mtt_{pc}}\right)^2 - 1\right] \cdot \sigma_{pc}^2 \tag{13}$$

$$\delta_{ei} = \left[\left(1 + \frac{mtt_{ei}}{mtt_{pc}}\right)^3 - 1\right] \cdot \delta_{pc} \tag{14}$$

in order to derive estimates for pulmonary capillary *mtt* (mtt_{pc}), variance (σ_{pc}^2), and skewness (δ_{pc}) for each extravascular indicator (e_i).

Figure 1b shows a model with two lumped, parallel pathways interposed between a pre-tissue injection site and a post-tissue/capillary sampling site; the heterogeneous circulation found in many organs is most simply described by two parallel pathways. The corresponding Erlang distribution is:

$$C(t) = A_1 \cdot \frac{k_1^{n_1} \cdot t^{n_1 - 1}}{(n_1 - 1)!} \cdot e^{-k_1 t} + A_2 \cdot \frac{k_2^{n_2} \cdot t^{n_2 - 1}}{(n_2 - 1)!} \cdot e^{-k_2 t} \tag{15}$$

or

$$C(t) = A_1 \cdot f_1(t) + A_2 \cdot f_2(t) \tag{16}$$

where the AUC is A_1 plus A_2 and the fractional flow through each pathway is the respective fractional AUC:

$$p = \frac{A_1}{A_1 + A_2} \quad \text{and} \quad q = \frac{A_2}{A_1 + A_2} \tag{17}$$

with $p + q = 1$.

The system *mtt* is calculated using the first moment of the function describing the drug concentration vs. time relationship:

$$mtt = \int_0^\infty t \cdot f(t)\, dt \tag{18}$$

but for a system with two parallel pathways, the *mtt* for the system is the sum of the flow-weighted *mtt*s for the individual circuits:

$$f(t) = p \cdot f_1(t) + q \cdot f_2(t) \tag{19}$$

$$mtt = p \cdot mtt_1 + q \cdot mtt_2 \tag{20}$$

In addition to the contributions of the variance seen in each pathway, one must consider the additional variance contributed by the relative separation of the *mtt*s in order to obtain the system's variance. Thus, the system

variance (or second central moment) in general is:

$$\sigma^2 = \int_0^\infty (t - mtt)^2 \cdot f(t)\, dt \tag{21}$$

and for two parallel paths:

$$\sigma^2 = \int_0^\infty [t - (p \cdot mtt_1 + q \cdot mtt_2)]^2 \cdot [p \cdot f_1(t) + q \cdot f_2(t)]\, dt \tag{22}$$

which, after integration, can be reduced algebraically to:

$$\sigma^2 = p\sigma_1^2 + q\sigma_2^2 + pq(mtt_2 - mtt_1)^2 \tag{23}$$

For skewness of the overall parallel system, one must also consider the additional skewness contributed by the separation of the individual *mtt*s and variances. In general, skewness (or third central moment) is defined as:

$$\delta = \int_0^\infty (t - mtt)^3 \cdot f(t)\, dt \tag{24}$$

and for two parallel paths:

$$\delta = \int_0^\infty [t - (p \cdot mtt_1 + q \cdot mtt_2)]^3 \cdot [p \cdot f_1(t) + q \cdot f_2(t)]\, dt \tag{25}$$

which, after integration, can be reduced algebraically to:

$$\delta = p\delta_1 + q\delta_2 + pq[(p - q)(mtt_2 - mtt_1)^3 + 3(\sigma_2^2 - \sigma_1^2)(mtt_2 - mtt_1)] \tag{26}$$

Arterial drug/marker concentration vs. time data prior to recirculation were fitted to a single and the sum of two gamma distributions using TableCurve2D ver 3.0 (Jandel Scientific, San Rafael, California) on a Pentium-based PC using constant standard deviation weighting. Model selection between single or dual pathway models was made on the bases of visual inspection of fit quality, adjusted r^2, and Akaike information criteria (AIC). The values of n_1 and n_2 were then rounded to the nearest integer and the data were fit to a single or the sum of two Erlang distributions [Eqs. (4) and (16)] to derive the parameters for the equivalent compartmental flow models. The effect of recirculation of a suddenly injected intravascular marker, such as ICG, is not evident until the marker concentration has nearly returned to baseline: monoexponential extrapolation from a point of the downlimb of the first-pass data at a time when the baseline is being approached, but prior to a time when any decrease in slope is evident, assures that recirculated indicator is not being included in the first-pass concentration history (12). Since the downlimb of a gamma distribution

function is a monoexponential decay, we applied these classical criteria for defining first-pass data to our analysis of data with the gamma and Erlang distribution functions.

Two sets of Eqs. (13) and (14) (one for each extravascular marker, antipyrine and alfentanil) were fitted simultaneously using the nonlinear, least-squares fitting routine of SAAM II (SAAM Institute, Seattle, Washington). Mean values for the estimates of pulmonary capillary transit were derived using a naive pooled data technique in which data from all four dogs were simultaneously fit to a single model using relative reciprocal weighting as the square of the reciprocal of the standard deviation (*SD*) of the observed data, assuming a fractional *SD* of 0.2.

A functional RBC/plasma partition ratio for antipyrine and alfentanil can be estimated from Eq. (8) and the relationship that blood indicator concentration is equal to the sum of the concentrations in plasma and RBCs weighted for their respective fraction of blood volume. The product of the cardiac output and the AUC for the plasma concentration vs. time curve equals dose when the RBC/plasma partitioning for the indicator is unity. From these relationships, a functional estimate of the RBC/plasma partition for an indicator or drug can be determined from *in vivo* data according to the following formula:

$$\frac{\text{RBC}}{\text{plasma}} = \frac{\text{Adm. Dose}}{\text{AUC} \cdot C.O. \cdot \text{Hct}} - \frac{1 - \text{Hct}}{\text{Hct}} \tag{27}$$

Estimates of the RBC/plasma partition coefficient thus derived should be considered functional in that they satisfy best the assumptions of the multiple indicator dilution technique in each study. The advantage of using a RBC/plasma partition ratio determined *in vivo* needs to be tempered by the consideration of the many possible confounding factors that may affect estimation of the first-pass AUC.

RESULTS

Figures 2a–d show the measured concentration histories and fitted single gamma or Erlang distributions (the fitted gamma and Erlang functions are indistinguishable so only a single line is shown) for all three indicators in all four dogs and Figs. 3a–d show the results for the sum of two gamma or Erlang distributions. Note that the single gamma or Erlang fits have systematic errors (Figs. 2a–d), suggesting model misspecification that does not exist in the double gamma or Erlang distribution (Figs. 3a–d). The selection of the double gamma distribution model over the single gamma distribution model was further based on improvement in adjusted r^2 and AIC. The average improvements in adjusted r^2 for the ICG, antipyrine, and

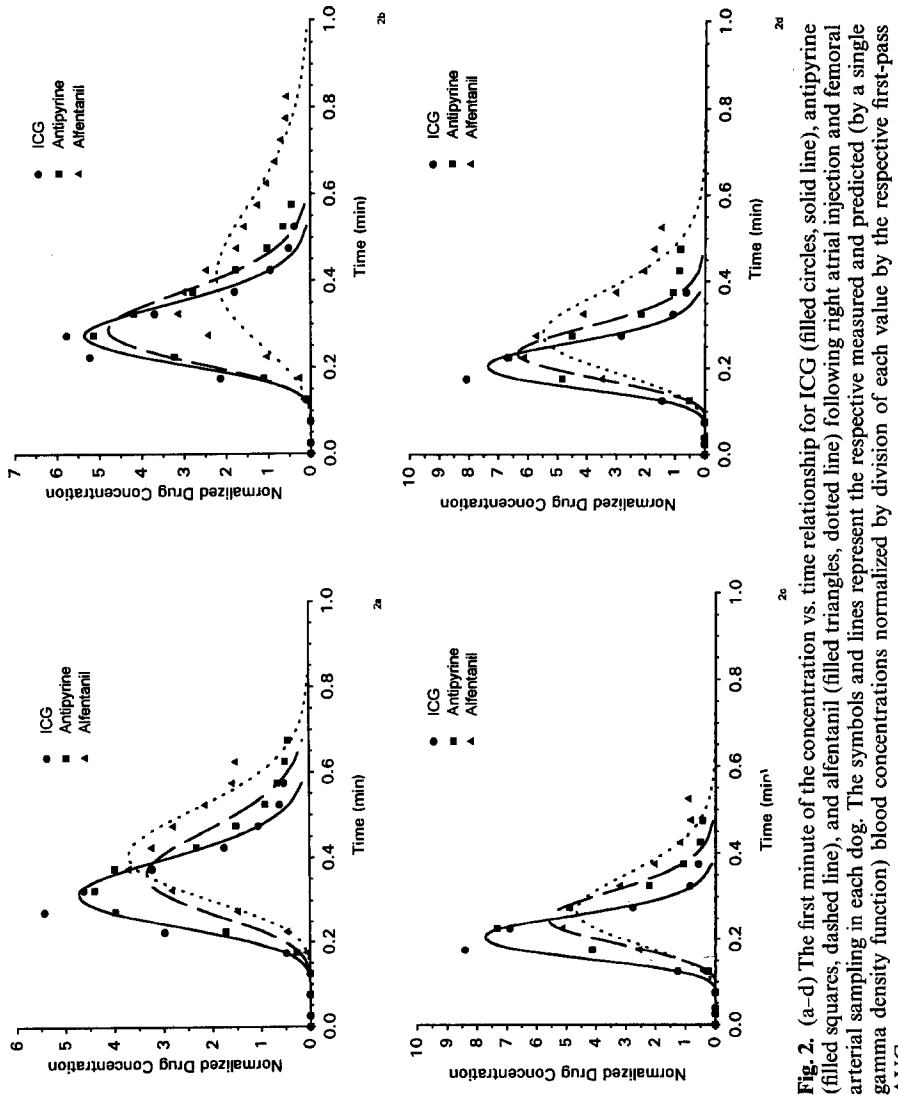

Fig. 2. (a–d) The first minute of the concentration vs. time relationship for ICG (filled circles, solid line), antipyrine (filled squares, dashed line), and alfentanil (filled triangles, dotted line) following right atrial injection and femoral arterial sampling in each dog. The symbols and lines represent the respective measured and predicted (by a single gamma density function) blood concentrations normalized by division of each value by the respective first-pass AUCs.

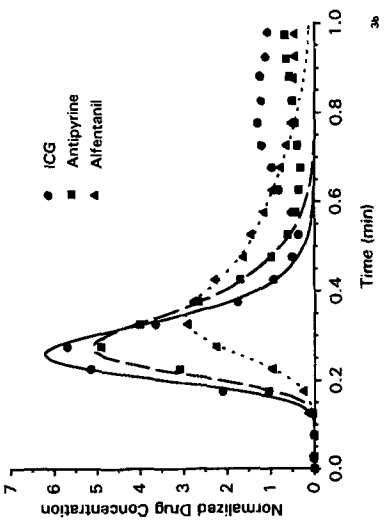

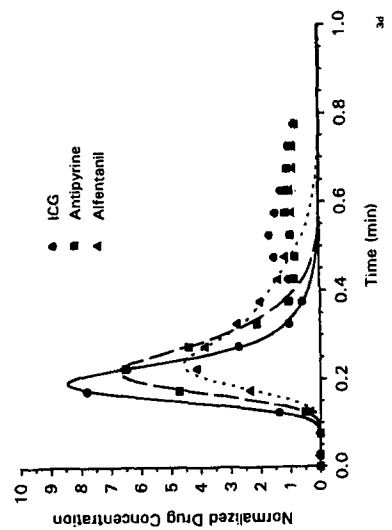

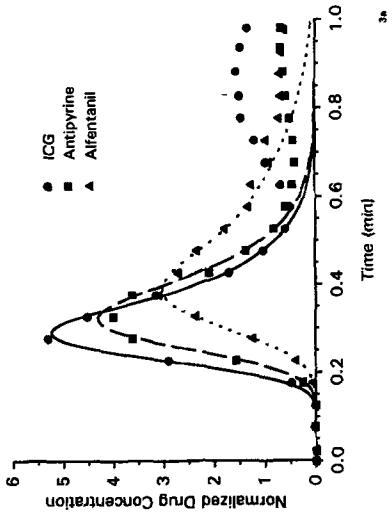

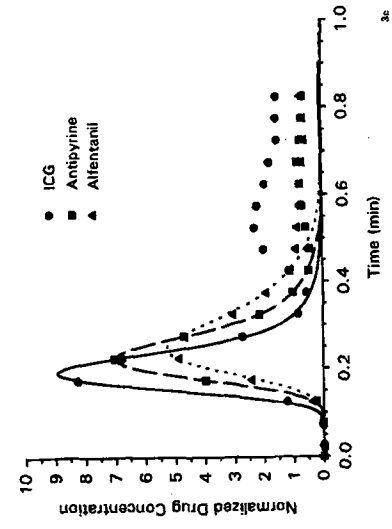

Fig. 3. (a–d) The first minute of the concentration vs. time relationship for ICG (filled circles, solid line), antipyrine (filled squares, dashed line), and alfentanil (filled triangles, dotted line) following right atrial injection and femoral arterial sampling in each dog. The symbols and lines represent the respective measured and predicted (by the parallel Erlang, or gamma, density functions) blood concentrations normalized by division of each value by the respective first-pass AUCs. Additional measured blood concentrations are presented to demonstrate the recirculatory nature of the *in vivo* experiment.

alfentanil models were 1.5%, 2.3%, and 3.4%, respectively. The adjusted r^2 for the double gamma distribution models were 0.995 or higher while those for the single gamma model function were as low as 0.920. In no instance was the improvement in unadjusted r^2 between a sum of two gamma distributions vs. the sum of two Erlang distributions more than 0.004%, making the respective lines for the predicted functions in Figs. 3a–d appear superimposed. The AIC also supported the dual gamma distribution model over the single gamma model in all of the alfentanil data sets, all but one of the antipyrine data sets (dog 4), and all but one of the ICG data sets (dog 3).

Despite the significantly improved fits of the dual gamma distribution function models over that of the single gamma distribution function models, the standard error of the parameter estimates for the gamma functions with the longer MTT were often quite large with FSDs ranging from 0.23–4.7 for ICG, 1.1–3.7 for antipyrine, and 0.07–2.2 for alfentanil. The high variance associated with these parameters was not markedly affected by the number of data points, or the cut-off for recirculation of drug. Fitting simulated data (with random error) of these models, with no recirculation and up to 100 data points, showed some improvement in the FSDs of the parameters, but frequently they remained above unity. Examination of the correlation matrices showed positive and negative correlations of 0.9 and above for all parameters in many instances, suggesting that the model solutions may not be unique.

From Table I it can be seen that there is good agreement between the thermal dilution cardiac outputs and those obtained from the fitted ICG gamma or Erlang functions despite differing methodologies (heat content vs. dye), sampling protocols (continuous, or 0.3 Hz, temperature sensing in the pulmonary artery vs. 3 second collections from the femoral artery via a roller pump), and AUC estimation algorithms. From Eq. (27) the mean estimates for the RBC/plasma partitioning of antipyrine and alfentanil under these *in vivo* conditions were 0.87 and 0.46, respectively.

Table I. Subject Information Including Cardiac Output by Dye Dilution (ICG), Thermodilution (TD), Central Blood Volume (ICG), and Pulmonary Tissue Volume (Antipyrine)

	Hct	Wt (kg)	$C.O._{ICG}$ (L/min)	$C.O._{TD}$ (L/min)	Central blood Vol.[a] (L)	Pulm. tis. Vol.[b] (L)
Dog 1	0.38	25	1.89	1.89	0.626	0.058
Dog 2	0.37	22	1.98	1.86	0.564	0.074
Dog 3	0.42	30	3.70	3.64	0.796	0.146
Dog 4	0.35	30	2.81	2.77	0.568	0.134
Mean	0.38	26.8	2.60	2.54	0.638	0.103
$\pm SD$	0.03	4.0	0.85	0.85	0.109	0.044

[a]Calculated as the product of ICG *mtt* and *C.O.*
[b]Calculated as the product of antipyrine *mtt* and *C.O.* minus central blood volume.

Table II. Mean ± *SD* of Central Circulation Parallel Erlang Parameters, and the Composite *mtt*, Variance (Square Root), and Skewedness (Cube Root) for the Various Drugs and that Derived for the Capillary Blood

	ICG	Antipyrine	Alfentanil	Capillary Blood
n_1	22.5 ± 4.2	21.2 ± 6.6	15.5 ± 2.6	—
k_1	116.1 ± 27.9	89.6 ± 23.8	60.0 ± 7.6	—
A_1	0.9 ± 0.4	5.8 ± 3.1	0.19 ± 0.05	—
n_2	13.0 ± 1.4	10.2 ± 3.2	6.5 ± 1.3	—
k_2	52.5 ± 12.9	33.4 ± 16.0	16.9 ± 6.0	—
A_2	1.1 ± 0.4	5.1 ± 3.8	0.34 ± 0.19	—
mtt (min)	0.23 ± 0.06	0.28 ± 0.06	0.35 ± 0.08	0.018 ± 0.010
variance (min)	0.066 ± 0.017	0.095 ± 0.032	0.15 ± 0.04	0.016 ± 0.015
skew (min)	0.16 ± 0.03	0.21 ± 0.05	0.28 ± 0.06	0.019 ± 0.020

In Table II are the parameter estimates of the sum of the first two Erlang functions derived from the least squares fits for all three drugs. These estimates were used to derive the means and standard deviations for the *mtt*, variance, and skewness of the first pass concentration vs. time curves for ICG, antipyrine, and alfentanil seen in Table II. It is readily apparent in Figs. 2 and 3 that the transit time through the central circulation and the lungs for ICG is less than that for antipyrine which, in turn, is less than that for alfentanil in all dogs. Subtracting the respective values for ICG from those for alfentanil and antipyrine, one obtains the *mtt*, variance and skewness for the extravascular concentration-time density function [Eqs. (10–12)]; the means and standard deviations are shown in Table II. In Fig. 4 the individual values for these extravascular parameters are plotted with the best fit of the functions delineated in Eqs. (13) and (14). The estimates of pulmonary capillary *mtt*, variance, and skewness derived from this fit appear in Table II.

DISCUSSION

The results of this analysis suggest that the considerable heterogeneity in the distribution of transit times in the pulmonary circulation may be described by two parallel, lumped pathways with different transit characteristics. Gamma and Erlang distributions perform equivalently in such a parallel system in their ability to characterize the lagged, right-skewed, first-pass drug concentration histories of multiple indicators. They also complement each other because they have mutually exclusive advantages. The sum of gammas is advantageous because the n parameters can be readily optimized, whereas the ns in the sum of Erlangs are not because most data-fitting software do not have parameter optimization algorithms restricted to integer increments. The sum of Erlangs is advantageous because it provides a means

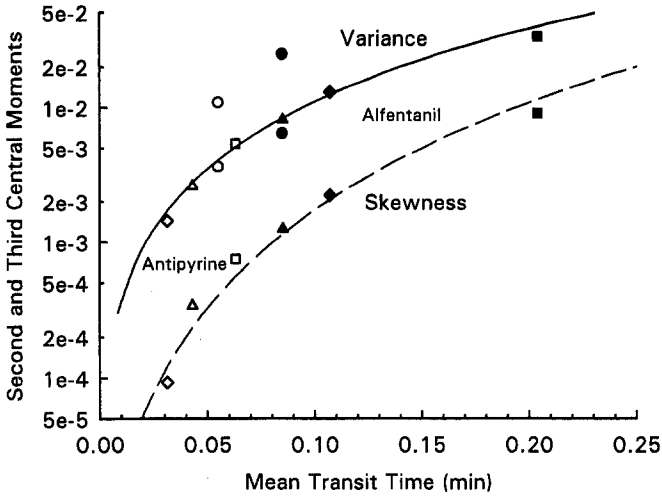

Fig. 4. The relationship of the extravascular mean transit time (abscissa) of antipyrine (open symbols) and alfentanil (closed symbols) vs. both the extravascular transit time variance (ordinate and upper symbols) and extravascular mean transit time skewness (ordinate and lower symbols) in each dog (dog 1, circles; dog 2, squares; dog 3, triangles; dog 4, diamonds). The upper solid line is predicted by the best fit of these data to Eq. (13) and the lower dashed line is that predicted by the best fit to Eq. (14). Note how the antipyrine values tend to cluster (pulmonary $mtt = 2$–4 min) while those of alfentanil tend to separate.

of incorporating the results of lagged, first-pass kinetics into a compartmental model of ordinary differential equations. Thus, this approach will enable incorporation of an accurate depiction of first-pass pulmonary kinetics into models describing the subsequent systemic disposition. These models can also be used to construct pharmacokinetic models which account for the first arterial appearance of drug in addition to systemic disposition.

Analysis of single-pass indicator dilution data obtained only from the tissue effluent, such as in this pulmonary first-pass study, requires a model with a time lag or delay because drug does not appear at the sampling site at the time of administration. A time lag is required when a model is incomplete because the subsystem that generates the lag has been omitted (3). The linear chain produces a distribution of lag times which is well-suited to describe drug distribution because laminar flow in the vasculature, turbulence at branch points, and the distribution of path lengths contribute to a continuous distribution of circulatory lags or transits. Time lags produced by chains of n compartments with the same transfer coefficient

(i.e., the Erlang distribution) provide very good approximations of the partial differential equation subsystem; as $n \to \infty$ the linear chain produces a discrete delay (3).

A linear compartmental chain (or tanks-in-series) was unable to characterize well the outflow from the isolated perfused liver (17). Comparison of mathematical organ perfusion models by Roberts *et al.* demonstrated that a single tanks-in-series model characterized hepatic outflow data with small, but systematic error, strongly suggesting model misspecification (17). Their analysis led them to advocate a parallel tubes model to better account for heterogeneity of organ transit times. We experienced similar difficulties (see Fig. 2a–d) when our pulmonary outflow data were fit with a single linear chain, or Erlang function, despite allowing n to vary during the curve fitting process. Resolution of our modeling difficulties with two parallel linear chains is analogous to the successful application of the parallel tube model to hepatic outflow data by Roberts *et al.* (17).

Roberts and Weiss have recently reported a stochastic modeling technique for tissue outflow of drug concentrations with a sampling density similar to that in the present study. As in the present study, these authors found that a mixture of two density functions gave the optimum fit to describe the dispersion of transit times. They used a mixture of two Gaussian functions rather than gamma or Erlang functions but did not report the standard errors of the parameter estimates nor the correlation between these parameters. We fit some of our current data to a sum of two Gaussian distribution functions and found the quality of the fits, the adjusted r^2, standard errors of the estimates, and the parameter correlations to be nearly identical to those obtained with two gamma functions. It should be noted that with both models, fit quality is high, but in some data sets parameter confidence is relatively low. This may be an indication that in some instances the precise parameter estimates may not be unique because of the high correlation between parameters. This condition should be considered when interpreting the significance of the individual density function making up the mixture.

Audi *et al.* have described a technique for analyzing multiple indicator (including alfentanil) data from an *in vitro* isolated lung preparation which can also determine pulmonary kinetics (4, 5). We have used their technique to analyze data from an *in vivo* study. The average capillary mean transit time, using an indirect technique, of 1.1 (±0.57) sec in the present study is in agreement with the reports of others. Audi *et al.* reported a mean of 3.18 sec in the isolated perfused dog lung using a multiple indicator dilution method (4). Capen *et al.* used both *in vivo* microscopy and diffusing capacity techniques to estimate pulmonary capillary transit times and obtained values

of 1.75 sec and 1.85 sec, respectively for the direct and indirect techniques (18). On the basis of a combined morphometric and indicator dilution technique, Hogg *et al.* reported a mean pulmonary capillary transit time of 1.37 sec with individual values in the range of 0.18 sec to 7.6 sec, depending on the region of the lung they investigated (19). A vertical gradient of mean pulmonary capillary transit times in different regions of the lung of anesthetized dogs has been reported by Wagner *et al.* who used a direct technique to determine mean times of 12.3 sec, 3.1 sec, and 1.6 sec for the upper, middle, and lower lung, respectively (20). Reduced blood flow in the upper lung in comparison to the gravity-dependent regions is reflected by fewer capillaries and longer transit times (20,21). Given these distributions of observed transit times, it is not surprising that these findings would be reflected in kinetic heterogeneity such as that seen in the present study. Others have proposed models with parallel heterogeneity to explain the distribution of flows and transit times in the pulmonary circulation (22,23) but it remains to be determined whether the distribution of transit times that we model define physiologic reality.

In their description of the estimation technique for capillary transit variables, Audi *et al.* (4) stated that the technique is not very robust when only two extravascular markers with flow-limited distribution are used in each experiment and suggested that improved parameter confidence could be obtained by increasing the number of markers. We also found parameter estimation to be unsatisfactory. Specifically, in one experiment we could not get convergence on a solution and in the others the fractional standard deviations (FSDs) for the parameter estimates all exceeded unity with many in excess of 2.0. Because we did not have the option of increasing the number of extravascular marker drugs, we instead combined the data from multiple experiments in a naive pooled data analysis technique in which the estimates of extravascular transit time, variance, and skewness for both drugs in all dogs were combined and fit simultaneously to a single model. We, therefore, cannot recommend that the technique be used *in vivo* with only two extravascular indicators in an experiment in which one wishes to estimate the capillary transit variables in an individual.

Detailed tissue drug uptake models are normally restricted to *in vitro* paradigms in order to both control drug administration and blood sampling and eliminate the confounding effect of recirculation. While the sites of drug administration and sampling for *in vivo* pulmonary tissue drug uptake studies can be controlled easily, the difficulty of recirculation remains. The dilemma presented by recirculation is most evident for a drug like alfentanil because its significant pulmonary uptake prolongs its mean transit time and broadens its first-pass peak (i.e., increases its variance). Blood ICG begins to recirculate during the early downstroke of the initial

alfentanil appearance curve (Figs. 3a–d), therefore, beginning at this point, alfentanil disposition includes both first-pass and recirculation data. In cases in which the pulmonary uptake of the drug of interest is extensive, hence recirculation occurs relatively quickly, the present modeling technique will be able to characterize the curve accurately but may not yield estimates that would be valid for characterizing details of pulmonary uptake with a single sampling site.

Simple examination of the primary concentration vs. time data may be insufficient to determine conclusively whether a particular data set will yield meaningful parameters for the description of pulmonary drug disposition. We have followed the procedure of previous investigators (1,2) and excluded drug concentration data when there was evidence of drug recirculation. This data rejection procedure would be expected to result in a poor characterization of the actual shape of the first-pass drug concentration history (loss of later portions with longer half-lives, yielding underestimation of AUC) for drugs with longer mean transit times due to their high pulmonary uptake. Based on studies in an isolated, perfused rat hindlimb, Zhen *et al.* (24) has suggested that if the ratio of the apparent dose, calculated as the product of blood flow and single-pass AUC, to the actual dose is less than 0.8, then the resultant kinetic parameter estimates related to tissue uptake (i.e., *mtt* and Vd) should be considered invalid. With poor dose recovery, two potentially important processes remain uncharacterized: actual elimination by the studied organ or the presence of a large, slowly equilibrating compartment. Even under conditions without recirculation and relatively long outflow sampling periods, more than 20% of certain basic drugs (e.g., propranolol) were retained within the tissue. In the present study in which plasma rather than blood concentrations were determined, Eq. (27) was used to estimate relative drug recovery.

The blood/plasma partition coefficient of 0.7 for alfentanil in rats reported by Björkman *et al.* (25) corresponds to an RBC/plasma partition ratio of 0.33, assuming a hematocrit of 0.45. Using 0.33 as the RBC/plasma partition ratio it would be expected that the alfentanil dose calculated as the product of the plasma AUC and cardiac output would be 1.33 mg. This corresponds well with the 1.28 ± 0.16 mg observed in the present study and indicates that alfentanil pulmonary tissue distribution was well characterized and that significant metabolism in pulmonary tissue is unlikely. Similarly, based on a RBC/plasma partition ratio of 0.82 reported for dogs by Clausen *et al.* on the basis of standard *in vitro* equilibration techniques (26), one would expect a plasma apparent antipyrine dose recovery of 26.8 mg. Again, this corresponds well with the 26.7 ± 3.0 mg observed in the present study and is consistent with the ability of first-pass antipyrine data to adequately characterize pulmonary tissue distribution (26).

The pulmonary capillary transit analyses make use of the higher order moments of the first-pass outflow curves, Eqs. (13) and (14). Because it is the nature of these higher order moments to be heavily time-weighted, one might expect that any error introduced by model extrapolation beyond the data, necessitated by recirculation, would be maximally exposed in this analysis. In Fig. 4 it is apparent that the antipyrine extravascular *mtt*s vary only slightly among the dogs, whereas those for alfentanil are more widely separated. Possible alternate interpretations of these results are that the pulmonary tissue interaction of alfentanil is more variable than that of antipyrine or that there is a greater degree of uncertainty in the higher order moments of alfentanil because its longer *mtt*s compared to antipyrine results in greater portions of its first-pass curves being in the extrapolated segments. This is consistent with the FSDs associated with the parameter estimates of the pulmonary capillary transit analysis in which the FSD of skew > variance > MTT (Table II). Nevertheless, the problem of model extrapolation beyond the data does not appear to affect greatly the ability of these *in vivo* data to estimate pulmonary capillary kinetics as these results (see Table II) agree with more direct observations of others in dogs (4). However, further analysis with a nonrecirculating system would be required to determine rigorously the significance of these issues.

We have developed a pharmacokinetic technique that can be used to characterize the first-pass arterial concentration vs. time relationship for multiple drugs or markers given by right artrial bolus injection. This model has two parallel linear chains (or tanks-in-series) and directly corresponds to a sum of two Erlang or gamma distributions. The Erlang and gamma functions are convenient because they characterize the lagged, right-skewed frequency distributions that are typical of plasma drug concentration histories obtained from single-pass tissue distribution studies and because higher-order moments are readily calculated from the primary parameters. We have provided the algebraic derivations that are needed to calculate the higher order moments for a system of two parallel pathways. Finally, we have shown that data obtained *in vivo* and analyzed using these techniques provides reasonable physiologic estimates of cardiac output, thoracic blood volume, pulmonary extravascular water, and the distribution of pulmonary capillary transit times. Furthermore, it may provide a tool for investigating the variability in pulmonary uptake of a drug among individuals. Our results suggest that comparison of *in vivo* and *in vitro* RBC/plasma drug partitioning and examination of an analysis of pulmonary capillary kinetics may help resolve whether kinetic estimates of a drug's apparent pulmonary tissue *mtt* and pulmonary distribution volume, determined from first-pass data, are valid. This approach should prove useful in the examination of the physiologic basis of differences in drug response during and following rapid intravenous infusion, particularly if there is significant pulmonary uptake.

REFERENCES

1. C. Post. Studies on the pharmacokinetic function of the lung with special reference to lidocaine. *Acta Pharmacol. Toxicol. (Copenh)* **1**:1–53 (1979).
2. D. L. Roerig, K. J. Kotrly, C. A. Dawson, S. B. Ahlf, J. F. Gualtieri, and J. P. Kampine. First-pass uptake of verapamil, diazepam, and thiopental in the human lung. *Anesth. Anal.* **69**:461–466 (1989).
3. J. A. Jacquez. *Compartmental Analysis in Biology and Medicine*, Second Ed., The University of Michigan Press, Ann Arbor, 1985.
4. S. H. Audi, G. S. Krenz, J. H. Linehan, D. A. Rickaby, and C. A. Dawson. Pulmonary capillary transport function from flow-limited indicators. *J. Appl. Physiol.* **77**:332–351 (1994).
5. S. H. Audi, J. H. Linehan, G. S. Krenz, C. A. Dawson, S. B. Ahlf, and D. L. Roerig. Estimation of the pulmonary capillary transport function in isolated rabbit lungs. *J. Appl. Physiol.* **78**:1004–1014 (1995).
6. T. K. Henthorn, M. J. Avram, T. C. Krejcie, C. A. Shanks, and D. A. Kaczynski. Minimal compartmental model of circulatory mixing of indocyanine green. *Am. J. Physiol.* **262**:H903–H910 (1992).
7. T. C. Krejcie, T. K. Henthorn, C. A. Shanks, and M. J. Avram. A recirculatory model describing the circulatory mixing, tissue distribution and elimination of antipyrine in dogs. *J. Pharmacol. Exp. Ther.* **269**:609–619 (1994).
8. Y. F. Huang, R. N. Upton, L. E. Mather, and W. B. Runciman. An assessment of methods for sampling blood to characterize rapidly changing blood drug concentrations. *J. Pharm. Sci.* **80**:847–851 (1991).
9. D. M. Grasela, M. L. Rocci, and P. H. Vlasses. Experimental impact of assay-dependent differences in plasma indocyanine green concentration determinations. *J. Pharmacokin. Biopharm.* **15**:601–613 (1987).
10. M. J. Avram and T. C. Krejcie. Determination of sodium pentobarbital and either sodium methohexital or sodium thiopental in plasma by high performance liquid chromatography with ultraviolet detection. *J. Chromatogr.* **414**:484–491 (1987).
11. S. Björkman and D. R. Stanski. Simultaneous determination of fentanyl and alfentanil in rat tissue by capillary gas chromatography. *J. Chromatogr.* **433**:95–104 (1988).
12. K. L. Zierler. Circulation times and the theory of indicator-dilution methods for determining blood flow and volume. In W. F. Hamilton (ed.), *Handbook of Physiology, Circulation, Vol. 1*, Section 2, American Physiological Society, Washington, D.C., pp. 585–615, 1962.
13. W. O. Cua, G. Basset, F. Bouchonnet, R. A. Garrick, G. Saumon, and F. P. Chinard. Endothelial and epithelial permeabilities to antipyrine in rat and dog lungs. *Am. J. Physiol.* **258**:H1321–H1333 (1990).
14. E. M. Renkin. Effects of blood flow on diffusion kinetics in isolated perfused hind legs of cats: A double circulation hypothesis. *Am. J. Physiol.* **183**:125–136 (1955).
15. T. K. Henthorn, T. C. Krejcie, and M. J. Avram. The relationship between alfentanil distribution kinetics and cardiac output. *Clin. Pharmacol. Ther.* **52**:190–196 (1992).
16. S. Björkman, D. R. Wada, D. R. Stanski, and W. F. Ebling. Comparative physiological pharmacokinetics of fentanyl and alfentanil in rats and humans based on parametric single-tissue models. *J. Pharmacokin. Biopharm.* **22**:381–409 (1994).
17. M. S. Roberts, J. D. Donaldson, and M. Rowland. Models of hepatic elimination: Comparisons of stochastic models to describe residence time distributions and to predict the influence of drug distribution, enzyme heterogeneity, and systemic recycling on hepatic elimination. *J. Pharmacokin. Biopharm.* **16**:41–83 (1988).
18. R. L. Capen, L. P. Latham, and W. W. Wagner. Comparison of direct and indirect measurements of pulmonary capillary transit times. *J. Appl. Physiol.* **62**:1150–1154 (1987).
19. J. C. Hogg, B. A. Martin, S. Lee, and T. McLean. Regional differences in erythrocyte transit times in normal lungs. *J. Appl. Physiol.* **59**:1266–1271 (1985).
20. W. W. Wagner, Jr., L. P. Latham, W. L. Hanson, S. E. Hoffmeister, and R. L. Capen. Vertical gradient of pulmonary capillary transit times. *J. Appl. Physiol.* **61**:1270–1274 (1986).

21. J. C. Hogg, T. McLean, B. A. Martin, and B. Wiggs. Erythrocyte transit and neutrophil concentration in the dog lung. *J. Appl. Physiol.* **65**:1217–1225 (1988).
22. R. W. Glenny and H. T. Robertson. Fractal properties of pulmonary blood flow: characterization of spatial heterogeneity. *J. Appl. Physiol.* **69**:532–545 (1990).
23. G. S. Krenz, L. Jianming, C. A. Dawson, and J. H. Linehan. Impact of parallel heterogeneity on a continuum model of the pulmonary arterial tree. *J. Appl. Physiol.* **77**:660–670 (1994).
24. Y. W. Zhen, S. E. Cross, and M. S. Roberts. Influence of physicochemical parameters and perfusate flow rate on the distribution of solutes in the isolated perfused rat hindlimb determined by the impulse-response technique. *J. Pharm. Sci.* **84**:1020–1027 (1995).
25. S. Björkman, D. R. Stanski, D. Verrotta, and H. Harashima. Comparative tissue concentration profiles of fentanyl and alfentanil in humans predicted from tissue/blood partition data obtained in rats. *Anesthesiology* **72**:865–873 (1990).
26. G. Clausen, A. Hope, and K. Aukland. Partition of ^{125}I-iodoantipyrine among erythrocytes, plasma and renal cortex in the dog. *Acta Physiol. Scand.* **107**:63–68 (1979).